Biochemical and Biophysical Research Communications 416 (2011) 277–282

Contents lists available at SciVerse ScienceDirect

Biochemical and Biophysical Research Communications

journal homepage: www.elsevier.com/locate/ybbrc

Expression and characterization of recombinant kurtoxin, an inhibitor of T-type voltage-gated calcium channels

Chul Won Lee [a,b], Young-Jae Eu [a], Hye Jung Min [a], Eun-Mi Cho [a], Jun-Ho Lee [c], Ha Hyung Kim [d], Seung-Yeol Nah [c], Kenton J. Swartz [e], Jae Il Kim [a,*]

[a] Department of Life Science, Gwangju Institute of Science and Technology (GIST), Gwangju 500-712, Republic of Korea
[b] Department of Chemistry, Chonnam National University, Gwangju 500-757, Republic of Korea
[c] Department of Physiology, College of Veterinary Medicine, Konkuk University, Seoul 143-701, Republic of Korea
[d] College of Pharmacy, Chung-Ang University, Seoul 156-756, Republic of Korea
[e] Molecular Physiology and Biophysics Section, National Institute of Neurological Disorders and Stroke, National Institute of Health, Bethesda, MD 20892, USA

ARTICLE INFO

Article history:
Received 28 October 2011
Available online 10 November 2011

Keywords:
Kurtoxin
Scorpion toxin
T-type calcium channel
Disulfide bond

ABSTRACT

Kurtoxin, a 63-amino acid peptide stabilized by four disulfide bonds, is the first reported peptide inhibitor of T-type voltage-gated calcium channels. Although T-type calcium channels have been implicated in a number of disease states, including epilepsy, chronic pain, hypertension and cancer, the lack of selective inhibitors has slowed progress in understanding their precise roles. Kurtoxin is a potentially valuable tool with which to study T-type calcium channels. However, because of the limited availability of the native protein, little is known about the structure and molecular mechanism of kurtoxin. Here we report the expression of kurtoxin in *Escherichia coli* and the structural and functional characterization of the recombinant protein. The disulfide bond pairings and secondary structure of recombinant kurtoxin were characterized through enzymatic cleavage, mass analysis and CD spectroscopy. Recombinant kurtoxin almost completely inhibited the T-type calcium channel in a manner identical to the native toxin. The availability of recombinant kurtoxin that is identical to the native toxin should help in the study of T-type calcium channels and enable development of new strategies for producing even more-selective T-type calcium channel inhibitors and for investigating the molecular basis of the toxin-channel interactions.

1. Introduction

Voltage-gated calcium channels are crucial regulators of intracellular calcium concentrations in a variety of cells, and have been classified into several subtypes based on their electrophysiological and pharmacological properties [1–4]. Peptide toxins from animal venoms have become valuable tools with which to functionally classify ion channels. For example, N-type calcium channels are selectively inhibited by ω-conotoxins GVIA and MVIIA, isolated from the venom of marine *Conus* snails, while P-type calcium channels are specifically blocked by ω-agatoxin IVA from the venom of the funnel web spider *Agelenopsis aperta*, and P/Q-type channels are blocked by ω-conotoxins MVIIC and TxVII [5,6]. Although peptide toxins are diverse, their modes of action fall into two major categories. Pore-blocking toxins, such as ω-conotoxin GVIA, bind to the external vestibule of the channel and physically obstruct the movement of ions by occluding the ion-conducting pore (7–10). On the other hand, gating modifiers, like ω-agatoxin IVA, bind close to the channel voltage sensor and alter the energetics of voltage-dependent gating [7–16].

Kurtoxin, isolated from the venom of the scorpion *Parabuthus transvaalicus*, is the first peptide ligand known to act with high affinity on T-type calcium channels expressed in *Xenopus* oocytes, and to distinguish between T-type calcium channels and other calcium channel subtypes, including the N-, P/Q-, and R-types [17]. Although T-type calcium channels are involved in a number of pathophysiological processes, including epilepsy, chronic pain, congestive heart failure and hypertension, details of their function remain largely unknown [12,13]. This is in part due to a lack of selective T-type calcium channel inhibitors. Kurtoxin is thus a potentially valuable tool with which to study T-type calcium channels.

Kurtoxin shows high sequence identity with the α-scorpion toxins that target Na^+ channels, including Cse-V, AaH II and BmK M1.

Abbreviations: C, cysteine; CD, circular dichroism; IPTG, isopropyl β-D-thiogalactoside; MALDI-TOF MS, matrix-assisted laser desorption/ionization-time of flight mass spectrometry; NMR, nuclear magnetic resonance; PCR, polymerase chain reaction; RP-HPLC, reverse-phase high-performance liquid chromatography; SDS–PAGE, sodium dodecyl sulfate–polyacrylamide gel electrophoresis; TFA, trifluoroacetic acid.

* Corresponding author. Fax: +82 62 970 2553.
E-mail address: jikim@gist.ac.kr (J.I. Kim).

0006-291X/$ - see front matter © 2011 Elsevier Inc. All rights reserved.
doi:10.1016/j.bbrc.2011.11.003

And like the α-scorpion toxins, kurtoxin interacts with voltage-activated Na^+ channels and slows their inactivation [17,18]. On the basis of these functional similarities, we presume the three-dimensional structure of kurtoxin is in some ways similar to that of α-scorpion toxins. However, the inhibition of T-type calcium channels by kurtoxin distinguishes it from other α-scorpion toxins and implies the presence of key structural differences that enable it to recognize that channel. In the present report, we describe the expression of recombinant kurtoxin in *Escherichia coli* and the characterization of its disulfide pairing and secondary structure.

2. Materials and methods

2.1. Plasmid construction

An artificial kurtoxin gene was made from overlapping single-stranded oligonucleotides designed for *E. coli* codon preference (Fig. 1A) and amplified by PCR using the primer pair CCATGAAAATC-GACGGCTACCCGGTG and CCGCTCGAGTCACGCACGG. The PCR product was purified and cloned into a pGEM-T easy PCR cloning vector. The EcoRI-digested insert was then ligated into the *E. coli* protein expression vector pRSET C (Invitrogen, USA), yielding the kurtoxin expression vector pRSET-ktx.

2.2. Preparation of linear kurtoxin

E. coli BL21 (DE3) cells were transformed with the plasmid pRSET-ktx and cultured at 37 °C in LB medium in the presence of

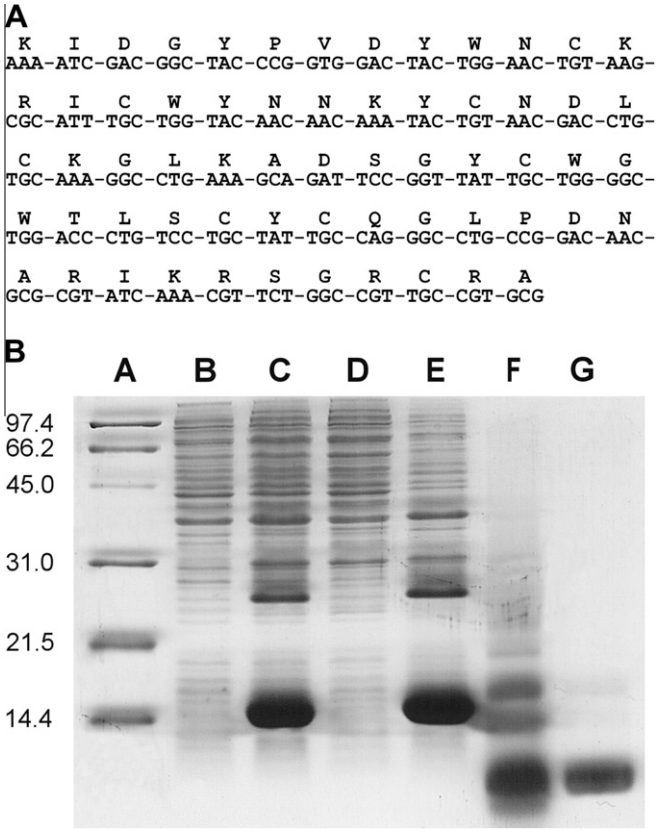

Fig. 1. (A) Design of the synthetic kurtoxin gene. Shown is the DNA sequence of the synthetic gene and the corresponding amino acid sequence. (B) Profile of the kurtoxin expression in *E. coli*. Coomassie blue stained 15% SDS–PAGE showing the following: lane A, molecular weight markers (kDa); lane B, extract of uninduced *E. coli* containing the pRSET-ktx expression vector; lane C, extract of IPTG-induced *E. coli* containing the vector; lanes D and E, supernatant (D) and pellet (E) fractions of the induced extract; lanes F and G, before (F) and after (G) CNBr cleavage of the insoluble fraction.

100 μg/ml ampicillin. Fusion protein synthesis was induced in late log phase (OD600 = 1.0) by addition of isopropyl β-D-thiogalactoside (IPTG) to 1 mM. Chemical digestion of the N-terminal fusion protein was accomplished using CNBr according to the method of Gross [19] with some modification. The pelleted protein was suspended in 70% formic acid to a final protein concentration of 2 mg/ml, after which CNBr was added to a 100 times molar excess over the methionine residues in the protein. The protein was then lyophilized, dissolved in denaturation buffer (8 M urea, 50 mM dithiothreitol, 50 mM Tris–HCl, pH 8.0, 1 mM EDTA) and incubated for 12 h at room temperature. The denatured kurtoxin was purified by preparative reverse-phase high-performance liquid chromatography (RP-HPLC). All samples were then subjected on 15% sodium dodecyl sulfate polyacrylamide gel electrophoresis (SDS–PAGE).

2.3. In vitro oxidative folding and purification

The purified linear kurtoxin was solubilized and refolded in refolding solution [30% (v/v) acetonitrile, 100 mM ammonium acetate, 1 μM protein, 2 mM reduced glutathione, 0.2 mM oxidized glutathione, and pH 7.8] for 8 days at 4 °C, after which the crude oxidized products were purified by preparative RP-HPLC, and the purity of recombinant kurtoxin was confirmed by analytical RP-HPLC and MALDI-TOF MS measurements.

2.4. Electrophysiology of recombinant kurtoxin

Recombinant plasmids containing cDNA inserts for calcium channels were linearized by digestion with appropriate restriction enzymes. The cRNAs were then obtained from the linearized templates using an *in vitro* transcription kit (mMessage mMachine; Ambion, USA) with T7RNA polymerase. Oocytes were separated by treatment with collagenase and agitation for 2 h in Ca^{2+} -free medium containing 82.5 mM NaCl, 2 mM KCl, 1 mM $MgCl_2$, 5 mM HEPES, 2.5 mM sodium pyruvate, 100 units/ml penicillin and 100 mg/ml streptomycin. Stages V–VI oocytes were collected and stored in ND96 (96 mM NaCl, 2 mM KCl, 1 mM $MgCl_2$, 1.8 mM $CaCl_2$, and 5 mM HEPES, pH 7.5) supplemented with 0.5 mM the ophylline and 50 mg/ml gentamicin.

Two-electrode voltage-clamp recordings were obtained from single oocytes placed in a small Plexiglas net chamber (0.5 ml). The recordings were made at room temperature using a Geneclamp 500 amplifier (Axon Instruments, USA) and an Oocyte Clamp (OC-725C, Warner Instrument). The standard recording solution contained 20 mM $Ba(OH)_2$, 90 mM NaOH, 2 mM KOH, 5 mM HEPES and 300 μM niflumic acid.

2.5. Determination of disulfide bond pairings

Intramolecular disulfide bond pairings in kurtoxin were identified through sequential cleavage with proteases and MALDI-TOF MS measurements. Recombinant kurtoxin was first digested with trypsin (Promega, USA) in 50 mM Tris–HCl (pH 8.0). Each fragment was collected by RP-HPLC followed by treatment of chymotrypsin (Roche Applied Science, USA). The resultant mixture was subjected to RP-HPLC separation, and the major fragment was digested by endoproteinase D (Takara Bio Inc.) in 50 mM sodium phosphate buffer (pH 8.0). All purified fragments were analyzed by MALDI-TOF MS.

2.6. CD measurement and analysis

The kurtoxin CD spectrum was measured on a JASCO J-750 spectropolarimeter in 0.01 M sodium phosphate (pH 7.0) at 20 °C in a quartz cell with a 1-mm path length. The spectrum was expressed as molecular ellipticity [θ] in deg cm^2 $dmol^{-1}$.

The secondary structure of kurtoxin was then evaluated using the VARSELEC [20], selcon2 [21,22] and neural network [23] programs.

3. Result

3.1. Efficient expression of kurtoxin

To generate recombinant kurtoxin, *E. coli* BL21(DE3) cells were transformed with an artificial kurtoxin gene (Fig. 1A). Fig. 1B shows the sequence of the expressed fusion protein composed of kurtoxin and KSI fusion protein. The theoretical molecular weight of the fusion protein is 13.8 kDa, and a band of about 15 kDa appeared in the lane containing extracts from the transformed cells (Fig. 1B, lane C). As expected, this product was missing from the uninduced cells (Fig. 1B, lane B). Following centrifugation of the extract from the induced transformants, the recombinant fusion protein was found exclusively in the pellet fraction (Fig. 1B, lane E), and yield was approximately 30 mg/l of culture.

3.2. CNBr digestion and in vitro oxidative folding of linear kurtoxin

The insoluble fusion protein was washed using 0.5% (v/v) Triton X-100, after which the washed inclusion body was dissolved in 70% formic acid and cleaved with CNBr. On Coomassie blue-stained gels, the major fusion protein band at 14.4 kDa gradually disappeared over a period of 12 h as a protein band at 8 kDa developed (Fig. 1B, lane F). After 12 h the reaction mixture was lyophilized, and the protein was then dissolved in denaturing solution containing 8 M urea and 50 mM DTT. The resultant linear kurtoxin was collected by RP-HPLC and lyophilized. This preparation resolved as a single band on SDS–PAGE (Fig. 1B, lane G). The yield of linear kurtoxin was about 10 mg/l of culture.

Kurtoxin is rich in hydrophobic residues, which caused the denatured protein to aggregate when refolding was attempted under aqueous conditions. To determine the optimal conditions for refolding the purified linear kurtoxin, the process was carried out at various ionic strengths, temperatures and protein concentrations with different organic solvents and detergents, and was monitored by RP-HPLC. We found that the linear kurtoxin refolded with the best yield in 100 mM ammonium acetate buffer containing 2 mM reduced glutathione, 0.2 mM oxidized glutathione and 30% acetonitrile. The yield of the folded protein was about 2 mg/l of culture.

3.3. Characterization of recombinant kurtoxin

The purified recombinant kurtoxin was eluted as a single peak in ~30% (v/v) acetonitrile solution on RP-HPLC. Native kurtoxin had the same retention time; moreover, when a mixture of recombinant and native kurtoxin was applied to RP-HPLC, a single enlarged peak was eluted (Fig. 2), indicating that the recombinant and native proteins are identical. The molecular weight (7386.5 Da) of the eluted protein was consistent with the molecular weight (MH^+) of 7386.8 Da measured by MALDI-TOF MS.

The inhibitory effects of recombinant kurtoxin were examined using different types of voltage-gated calcium channels expressed on *Xenopus* oocytes (Fig. 3). The channel was activated for 200 ms every 10 s by applying depolarizing steps from a holding voltage of −80 mV. We found that at a concentration of 300 nM, the recombinant kurtoxin almost completely inhibited voltage-activated barium currents in oocytes expressing the α_{1G} T-type channel. By contrast, the same concentration of kurtoxin had no effect on α_{1A} (P/Q-type), α_{1B} (N-type), α_{1C} (L-type) or α_{1E} (R-type) channels, indicating the recombinant kurtoxin distinguishes between α_{1G} and other voltage-gated calcium channels in this expression system, similar to previous studies with native kurtoxin [17].

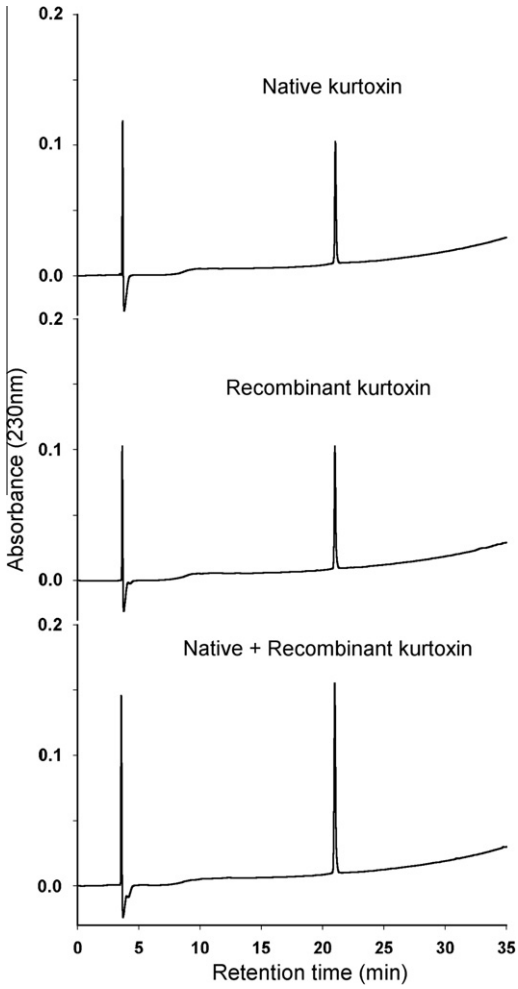

Fig. 2. Comparison of the RP-HPLC chromatographic behavior of native and recombinant kurtoxin. RP-HPLC chromatograms were recorded using an analytical RP-HPLC equipped with a 4.6 × 250 mm C18 silica column. Toxin was eluted with a linear gradient from 5% to 65% buffer B over 30 min at a flow-rate of 1 ml/min. See Section 2 for buffers A and B.

3.4. Disulfide bond parings of kurtoxin

Kurtoxin contains eight cysteines forming four disulfide bonds. Tryptic digestion of recombinant kurtoxin yielded two fragments, F1 and F2 (Fig. 4A). The F1 fragment eluted early (20% acetonitrile) on RP-HPLC and had a mass of 1948.5 Da. From the trypsin treatment, we determined that within this fragment the first cysteine (C1) forms a disulfide bond with the last (C8). The F2 fragment had a mass of 4358.5 Da and was composed of fragments connected by the remaining three disulfide bonds. We speculated that chymotrypsin digestion would isolate a link between C2 and C5, making fragment F3. After chymotrypsin treatment, we detected the F4 fragment, in which YCNDLCK was linked to TLSCY and CQGLPDNAR. The detection of F4 meant there was indeed a disulfide bond linking C2 and C5, but the mass of F3 was not found. By cleaving between C3 and C4 of YCNDLCK, we isolated the last disulfide bond. Endoproteinase D cut the peptide bond between the asparagine and aspartate of YCNDLCK, yielding the F5 fragment with a mass of 982.9 Da, indicating the presence of a disulfide bond between C3 and C6. The F6 fragment, with a mass of 993.6 Da

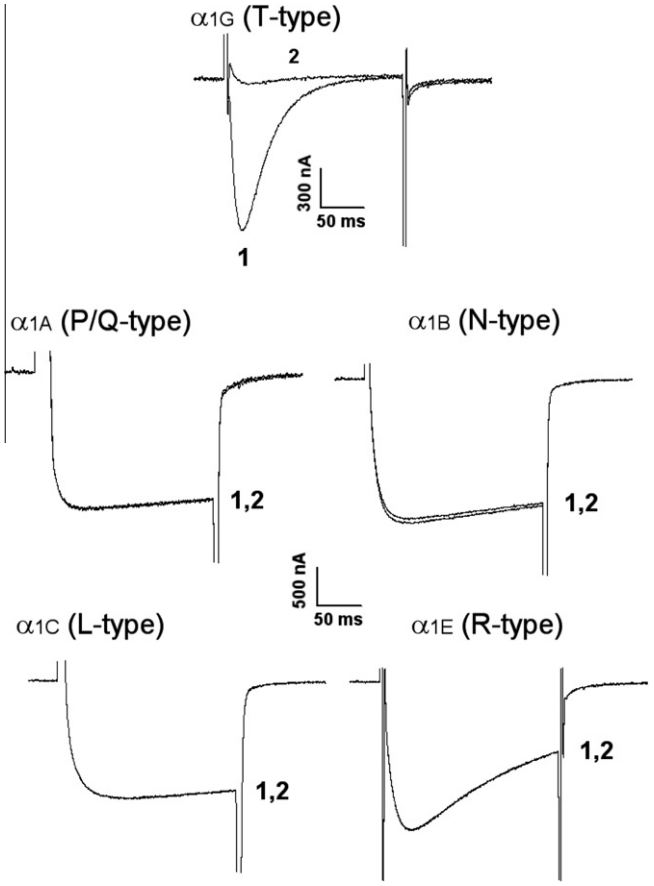

Fig. 3. Inhibition of α_{1G} T-type calcium channels by recombinant kurtoxin and its selectivity for different voltage-gated calcium channels. Superimposed traces were recorded in the absence (1) and presence (2) of 300 nM kurtoxin. Oocytes expressing the indicated calcium channel subtype were impaled with two microelectrodes filled with 3 M KCl (0.2–0.7 MΩ) and voltage-clamped at a holding potential of −80 mV. They were then depolarized for 200 ms every 10 s to +10 mV for P/Q-, N- and L-type channels, to 0 mV for R-type channels and to −20 mV for T-type channels.

resulting from a link between C4 and C7, was not detected. Thus the disulfide bond connectivities of kurtoxin are C1–C8, C2–C5, C3–C6 and C4–C7 (Cys^{12}–Cys^{61}, Cys^{16}–Cys^{37}, Cys^{23}–Cys^{44} and Cys^{27}–Cys^{46}).

3.5. Secondary structure of kurtoxin

The secondary structure of the recombinant kurtoxin was evaluated using circular dichroism (CD) spectroscopy (Fig. 4B). The obtained CD spectrum exhibited positive and negative Cotton effects around 198 and 207 nm, respectively, and a shoulder at around 220 nm. Using three fitting programs with the CD spectrum, we estimated the α-helix and β-sheet contents of kurtoxin to range from 11% to 17% and from 31% to 37%, respectively. The primary sequence of kurtoxin is similar to those of the α-scorpion toxins Cse-V, AaH II and BmK M1. The three-dimensional structures of Cse-V, AaH II and BmK M1 have been solved [24–26], and the α-helix contents are similar to that of kurtoxin, 15.8%, 15.6% and 15.6%, respectively. On the other hand, β-sheet contents of Cse-V, AaH II and BmK M1 are somewhat lower than that of kurtoxin, 23.8%, 25.0%, and 26.6%, respectively. This difference in the amount of β-sheet may reflect the different sources of data, one set from fitting the CD spectrum and the others from the three-dimensional structures, or may reflect local structural differences between kurtoxin and the other α-scorpion toxins.

4. Discussion

We have shown that kurtoxin can be efficiently expressed in a bacterial expression system, and have described the disulfide bridges and secondary structure of the recombinant protein. In general, short cysteine-rich peptides (<30 amino acids) can be chemically synthesized and folded *in vitro* with acceptable yields; with longer polypeptides (>30 amino acids), however, the yields become very low due to aggregation of the growing peptide within the reaction solvent during peptide synthesis [27]. Therefore, native chemical ligation was required to synthesize kurtoxin in a previous study [28]. In the present work, we expressed kurtoxin in *E. coli*, purified the toxin from inclusion bodies, and refolded the denatured polypeptide into the biologically active toxin in a hydrophobic solution (30% acetonitrile). The effect of the organic solvent on the folding of kurtoxin can likely be explained in terms of an isolating effect on the molecules that favors intramolecular disulfide bond formation. After refolding, the purified recombinant kurtoxin was identical to the native protein with respect to its RP-HPLC mobility, molecular weight and electrophysiological activity. Given that the amount of native kurtoxin that can be isolated is limited, the use of the recombinant toxin should help in the study of T-type calcium channels, as the recombinant approach will enable site-directed mutagenesis for analysis of the structure–activity relationships of kurtoxin.

To obtain information about the structure of kurtoxin, we determined the disulfide bond structure and analyzed its CD spectrum. The enzymatic digestion and mass measurements revealed that kurtoxin has the same disulfide bond pairings as other α-scorpion toxins and native kurtoxin [24–26,28–30]. Analysis of its CD spectrum showed that the structure of recombinant kurtoxin contains 11–17% α-helix and 31–37% β-sheet. This is similar to the CD spectrum of another α-scorpion toxin, BmK M1 [31]. Moreover, X-ray crystallographic analysis of BmK M1 revealed that its molecular fold adopts the classical conformation of α-scorpion toxins consisting of an α-helix and a triple-stranded antiparallel β-sheet stabilized by the four disulfide bridges (CSαβ motif) [24]. Although the atomic level structure of kurtoxin has not yet been solved, the CD studies supplemented by the disulfide bond structure suggest that the overall structure of kurtoxin is closely related with those of the α-scorpion toxins.

Kurtoxin has been characterized as a modifier of T-type calcium channel gating. We previously suggested that a surface motif comprised of a hydrophobic patch surrounded by positively charged residues is likely the region used by gating modifier toxins to bind to voltage-gated ion channels [32–34]. That linear kurtoxin formed aggregates under hydrophilic conditions but folded properly under hydrophobic solutions suggests it has a large hydrophobic region on its surface, and that it also adopts the gating modifier surface characteristics (hydrophobic patch) stabilized by an α-helix and β-sheet backbone framework.

Two striking characteristics of kurtoxin are its ability to shift the voltage-response relation of T-type calcium channels toward more positive potentials and to slow the inactivation of sodium channels, suggesting that the toxin interacts with the voltage sensors of the channel [35–39]. Although kurtoxin was first isolated as a specific T-type calcium channel inhibitor, it was later shown to affect the function of native voltage-gated L-, N- and P-type calcium channels in central and peripheral neurons [40]. These interesting differences in the way kurtoxin interacts with calcium channels expressed in oocytes compared to native neurons is intriguing, and may be due to the presence of auxiliary subunits

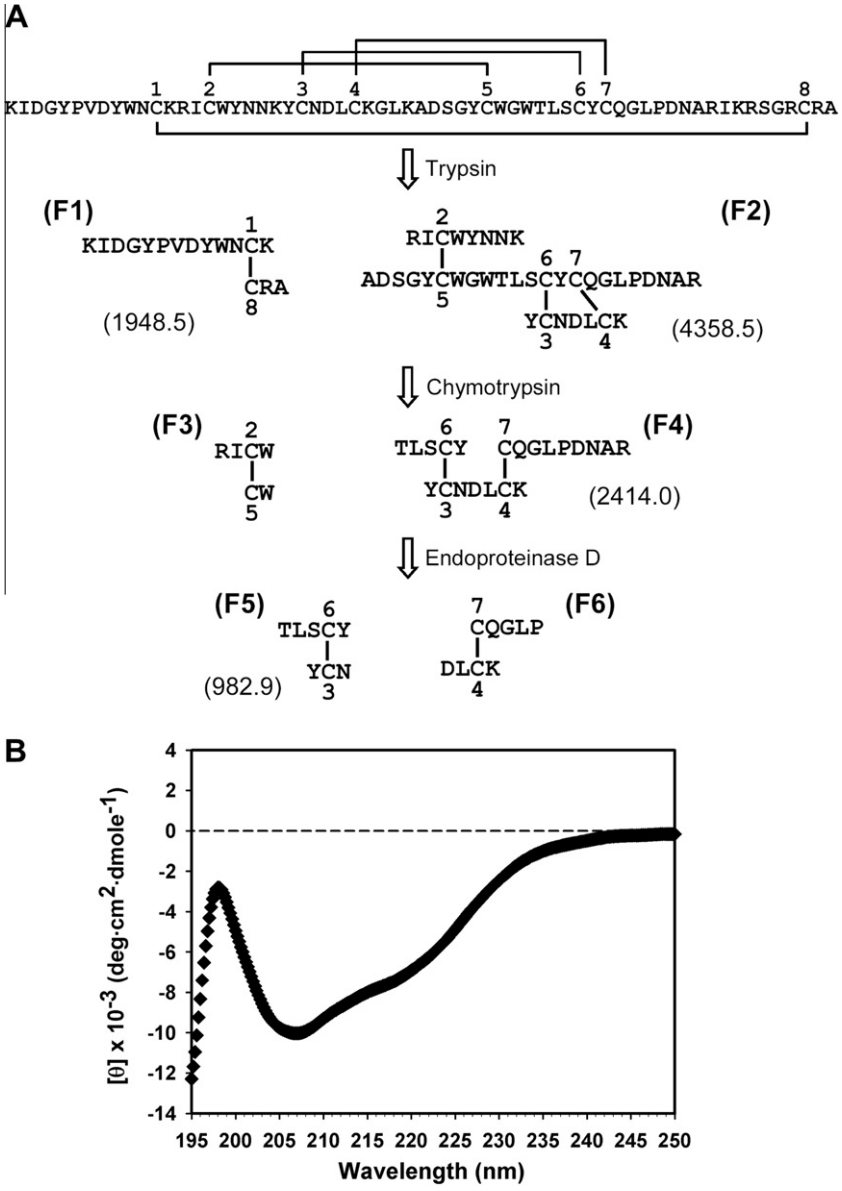

Fig. 4. (A) Scheme for identifying the intramolecular disulfide bonds in kurtoxin. Kurtoxin was sequentially cleaved with trypsin, chymotrypsin and endoproteinase D. The peptide fragments (F1–F6) released after each proteinase treatment were purified by RP-HPLC, and the molecular weight was measured by MALDI-TOF mass spectroscopy. The measured molecular weights of the enzymatic fragments are given in parentheses. (B) CD spectrum of recombinant kurtoxin. The CD spectrum was recorded in 0.01 M sodium phosphate (pH 7.0) at 20 °C.

in native neurons or different lipid membrane composition. The successful expression of the recombinant toxin reporter here will allow these differences to be explored in future studies. In addition site-directed mutagenesis of recombinant kurtoxin will facilitate the identification of variants with improved specificity, and investigation of the precise molecular mechanism by which kurtoxin interacts with calcium channels. To address these issues, site-directed mutagenesis of recombinant kurtoxin and determination of the three-dimensional structure by NMR spectroscopy are currently ongoing.

Acknowledgments

This research was supported by Grants from the Next-Generation BioGreen 21 Program (No. PJ008158), Rural Development Administration, Republic of Korea, the National Research Foundation of Korea Grant funded by the Korean Government (MEST) (NRF-C1ABA001-2011-0018559), the Brain Research Center of the 21st Century Frontier Research Program (M103KV010005-06K2201-00610), the BioImaging Research Center at the Gwangju Institute of Science and Technology, and Basic Research Projects in High-tech Industrial Technology funded by Gwangju Institute of Science and Technology in 2011.

References

[1] R.W. Tsien, P.T. Ellinor, W.A. Horne, Molecular diversity of voltage-dependent Ca^{2+} channels, Trends Pharmacol. Sci. 12 (1991) 349–354.
[2] E.A. Ertel, K.P. Campbell, M.M. Harpold, F. Hofmann, Y. Mori, E. Perez-Reyes, A. Schwartz, T.P. Snutch, T. Tanabe, L. Birnbaumer, R.W. Tsien, W.A. Catterall, Nomenclature of voltage-gated calcium channels, Neuron 25 (2000) 533–535.
[3] R.J. Miller, Voltage-sensitive Ca^{2+} channels, J. Biol. Chem. 267 (1992) 1403–1406.
[4] A. Randall, R.W. Tsien, Pharmacological dissection of multiple types of Ca^{2+} channel currents in rat cerebellar granule neurons, J. Neurosci. 15 (1995) 2995–3012.

[5] M. Fainzilber, J.C. Lodder, R.C. van der Schors, K.W. Li, Z. Yu, A.L. Burlingame, W.P. Geraerts, K.S. Kits, A novel hydrophobic omega-conotoxin blocks molluscan dihydropyridine-sensitive calcium channels, Biochemistry 35 (1996) 8748–8752.
[6] B.M. Olivera, G.P. Miljanich, J. Ramachandran, M.E. Adams, Calcium channel diversity and neurotransmitter release: the omega-conotoxins and omega-agatoxins, Annu. Rev. Biochem. 63 (1994) 823–867.
[7] E. Carbone, H.D. Lux, A low voltage-activated, fully inactivating Ca channel in vertebrate sensory neurones, Nature 310 (1984) 501–502.
[8] C.F. Chen, P. Hess, Mechanism of gating of T-type calcium channels, J. Gen. Physiol. 96 (1990) 603–630.
[9] M.C. Iftinca, G.W. Zamponi, Regulation of neuronal T-type calcium channels, Trends Pharmacol. Sci. 30 (2009) 32–40.
[10] L. Lacinova, Pharmacology of recombinant low-voltage activated calcium channels, Curr. Drug Targets: CNS Neurol. Disord. 3 (2004) 105–111.
[11] E. Bourinet, T.W. Soong, K. Sutton, S. Slaymaker, E. Mathews, A. Monteil, G.W. Zamponi, J. Nargeot, T.P. Snutch, Splicing of alpha 1A subunit gene generates phenotypic variants of P- and Q-type calcium channels, Nat. Neurosci. 2 (1999) 407–415.
[12] M. Hans, A. Urrutia, C. Deal, P.F. Brust, K. Stauderman, S.B. Ellis, M.M. Harpold, E.C. Johnson, M.E. Williams, Structural elements in domain IV that influence biophysical and pharmacological properties of human alpha1A-containing high-voltage-activated calcium channels, Biophys. J. 76 (1999) 1384–1400.
[13] S.I. McDonough, L.M. Boland, I.M. Mintz, B.P. Bean, Interactions among toxins that inhibit N-type and P-type calcium channels, J. Gen. Physiol. 119 (2002) 313–328.
[14] S.I. McDonough, I.M. Mintz, B.P. Bean, Alteration of P-type calcium channel gating by the spider toxin omega-Aga-IVA, Biophys. J. 72 (1997) 2117–2128.
[15] I.M. Mintz, V.J. Venema, K.M. Swiderek, T.D. Lee, B.P. Bean, M.E. Adams, P-type calcium channels blocked by the spider toxin omega-Aga-IVA, Nature 355 (1992) 827–829.
[16] J.R. Winterfield, K.J. Swartz, A hot spot for the interaction of gating modifier toxins with voltage-dependent ion channels, J. Gen. Physiol. 116 (2000) 637–644.
[17] R.S. Chuang, H. Jaffe, L. Cribbs, E. Perez-Reyes, K.J. Swartz, Inhibition of T-type voltage-gated calcium channels by a new scorpion toxin, Nat. Neurosci. 1 (1998) 668–674.
[18] H.L. Zhu, R.D. Wassall, T.C. Cunnane, N. Teramoto, Actions of kurtoxin on tetrodotoxin-sensitive voltage-gated Na+ currents, Na V1.6, in murine vas deferens myocytes, Naunyn Schmiedebergs Arch. Pharmacol. 379 (2009) 453–460.
[19] E. Gross, The cyanogen bromide reaction, Methods Enzymol. 11 (1967) 238–255.
[20] P. Manavalan, W.C. Johnson Jr., Variable selection method improves the prediction of protein secondary structure from circular dichroism spectra, Anal. Biochem. 167 (1987) 76–85.
[21] N. Sreerama, R.W. Woody, A self-consistent method for the analysis of protein secondary structure from circular dichroism, Anal. Biochem. 209 (1993) 32–44.
[22] N. Sreerama, R.W. Woody, Poly(pro)II helices in globular proteins: identification and circular dichroic analysis, Biochemistry 33 (1994) 10022–10025.
[23] M.A. Andrade, P. Chacon, J.J. Merelo, F. Moran, Evaluation of secondary structure of proteins from UV circular dichroism spectra using an unsupervised learning neural network, Protein Eng. 6 (1993) 383–390.
[24] X.L. He, H.M. Li, Z.H. Zeng, X.Q. Liu, M. Wang, D.C. Wang, Crystal structures of two alpha-like scorpion toxins: non-proline cis peptide bonds and implications for new binding site selectivity on the sodium channel, J. Mol. Biol. 292 (1999) 125–135.
[25] D. Housset, C. Habersetzer-Rochat, J.P. Astier, J.C. Fontecilla-Camps, Crystal structure of toxin II from the scorpion *Androctonus australis* Hector refined at 1.3 A resolution, J. Mol. Biol. 238 (1994) 88–103.
[26] M.J. Jablonsky, D.D. Watt, N.R. Krishna, Solution structure of an old world-like neurotoxin from the venom of the New World scorpion Centruroides sculpturatus Ewing, J. Mol. Biol. 248 (1995) 449–458.
[27] S.M. Hecht, Bioorganic Chemistry: Peptides and Proteins, Oxford University Press Inc., 1998.
[28] H. Nishio, Y. Nishiuchi, M. Ishimaru, T. Kimura, Chemical synthesis of kurtoxin, a T-type calcium channel blocker, Lett. Pept. Sci. 10 (2003) 589–596.
[29] I. Krimm, N. Gilles, P. Sautiere, M. Stankiewicz, M. Pelhate, D. Gordon, J.M. Lancelin, NMR structures and activity of a novel alpha-like toxin from the scorpion *Leiurus quinquestriatus* hebraeus, J. Mol. Biol. 285 (1999) 1749–1763.
[30] C. Landon, P. Sodano, B. Cornet, J.M. Bonmatin, C. Kopeyan, H. Rochat, F. Vovelle, M. Ptak, Refined solution structure of the anti-mammal and anti-insect LqqIII scorpion toxin: comparison with other scorpion toxins, Proteins 28 (1997) 360–374.
[31] Y.M. Sun, F. Bosmans, R.H. Zhu, C. Goudet, Y.M. Xiong, J. Tytgat, D.C. Wang, Importance of the conserved aromatic residues in the scorpion alpha-like toxin BmK M1: the hydrophobic surface region revisited, J. Biol. Chem. 278 (2003) 24125–24131.
[32] C.W. Lee, S. Kim, S.H. Roh, H. Endoh, Y. Kodera, T. Maeda, T. Kohno, J.M. Wang, K.J. Swartz, J.I. Kim, Solution structure and functional characterization of SGTx1, a modifier of Kv2.1 channel gating, Biochemistry 43 (2004) 890–897.
[33] H. Takahashi, J.I. Kim, H.J. Min, K. Sato, K.J. Swartz, I. Shimada, Solution structure of hanatoxin1, a gating modifier of voltage-dependent K(+) channels: common surface features of gating modifier toxins, J. Mol. Biol. 297 (2000) 771–780.
[34] K. Takeuchi, E. Park, C. Lee, J. Kim, H. Takahashi, K. Swartz, I. Shimada, Solution structure of omega-grammotoxin SIA, a gating modifier of P/Q and N-type Ca(2+) channel, J. Mol. Biol. 321 (2002) 517–526.
[35] Y. Jiang, A. Lee, J. Chen, V. Ruta, M. Cadene, B.T. Chait, R. MacKinnon, X-ray structure of a voltage-dependent K+ channel, Nature 423 (2003) 33–41.
[36] Y. Jiang, V. Ruta, J. Chen, A. Lee, R. MacKinnon, The principle of gating charge movement in a voltage-dependent K+ channel, Nature 423 (2003) 42–48.
[37] K.J. Swartz, R. MacKinnon, Mapping the receptor site for hanatoxin, a gating modifier of voltage-dependent K+ channels, Neuron 18 (1997) 675–682.
[38] K.J. Swartz, R. MacKinnon, Hanatoxin modifies the gating of a voltage-dependent K+ channel through multiple binding sites, Neuron 18 (1997) 665–673.
[39] K.J. Swartz, Tarantula toxins interacting with voltage sensors in potassium channels, Toxicon 49 (2007) 213–230.
[40] S.S. Sidach, I.M. Mintz, Kurtoxin, a gating modifier of neuronal high- and low-threshold ca channels, J. Neurosci. 22 (2002) 2023–2034.